Analysis of Vacuum Chamber Structure Based on Visual Finite Element Modeling

Yanhu Wang and Xizhang Chen

Abstract The feasibility of improving the vacuum chamber structure of vacuum packaging machine is discussed. The finite element software, Visual Environment, is used to simulate the structures of prime vacuum chamber and improved vacuum chamber which is built most through weld process. The results show that the maximum weld residual stress of the improved vacuum chamber changes and the stress concentration is greatly reduced with finite element analysis (FEA). At the same time, a path for a particular site is created and the range of stress changes is found from the original 270–340 to 240–310 MPa. The improved method not only saves resources but also improves product quality, which is verified by the actual product.

Keywords Vacuum chamber · Finite element analysis (FEA)
Welding residual stress · Structure

1 Introduction

With the improvement of modern consumption concept, product packaging and texture gradually arouse people's attention. The vacuum packaging compared to other packaging has the advantage to maintain the color and keep fresh in prolonged shelf-life items, especially for the packaging of active substances [1]. It promotes the evolution of the packaging machine. However, the vacuum packaging machine structure and the process designed by many enterprises are not much reasonable. Most of them lead the vacuum chamber to crack. A well-known packaging company named Hualian Machinery Group is good at producing the vacuum packaging machine. These years it also meets similar quality problem. In order to advance the vacuum packaging machine, it improves the structure of

Y. Wang · X. Chen (✉)
School of Mechanical and Electrical Engineering, Wenzhou University, Wenzhou, China
e-mail: kernel.chen@gmail.com

S. Chen et al. (eds.), *Transactions on Intelligent Welding Manufacturing*,
Transactions on Intelligent Welding Manufacturing,
https://doi.org/10.1007/978-981-10-7043-3_7

vacuum packaging machine. Consumers very satisfy the improvement vacuum packaging machine during the use of the product.

With the development of finite element technology, the product structure is constructed by the simulation to predict product defects and provide important information for structure optimization [2]. In this work, finite element analysis (FEA) software Visual Environment is used to analyze two different structures of vacuum chamber, and provides theoretical basis for the improvement on the vacuum chamber structure.

2 Vacuum Packaging Machine

2.1 Composition of the Vacuum Packaging Machine

The vacuum packaging machine is shown in Fig. 1. The vacuum packaging machine consists of handle, vacuum cover, link, seal assembly, vacuum chamber, chassis, control panels, vacuum pumps and caster. Eight main parts are shown in Table 1.

2.2 Working Principle

When the bag is in the vacuum chamber, the vacuum cover is closed, and the machine starts to build an airtight vacuum space. After vacuuming is completed, it

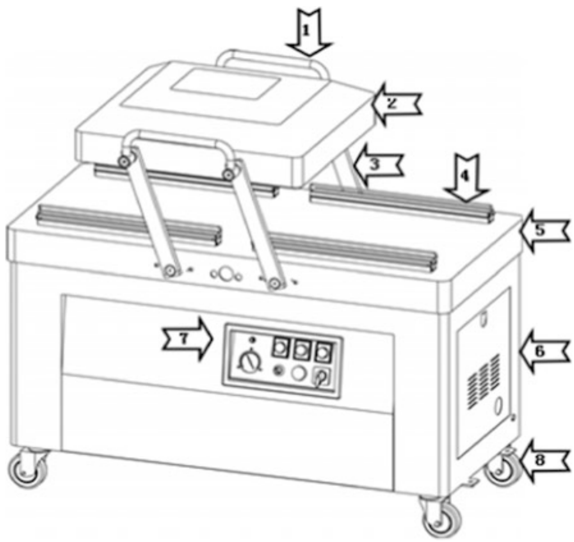

Fig. 1 Vacuum packaging machine

should fill with inert gas firstly if needed. Different pressure is used between the vacuum chamber and the outside atmosphere to overcome spring force. Let the heat sealing plate drop with the air bag. The heat sealing plate is installed with an electric hot flat. When there is a large low-voltage through the flat, heat is generated to seal the bag. The vacuum cover is cooled and then opened. At last, vacuum packaging process is completed.

3 FEA of Vacuum Chamber Model

3.1 Prime Machine's Vacuum Chamber

Material of vacuum chamber is 0Cr18Ni9 alloy. The composition is Cr18.09%, Ni8.15%, Si0.35%, C0.0344%, S0.003%, Mn1.03% and P0.039%, in addition to Fe. Table 2 shows some mechanical properties of 0Cr18Ni9 material. There are many studies on 0Cr18Ni9 stainless steel in stress corrosion, stress fatigue and fracture [3, 4]. When the material plastic deformation occurs, it is also prone to deformation which induces martensitic phase transformation. The formation of martensitic phase improves the strength and hardness of the material but reduces the ductility and toughness. Therefore, plastic deformation must be limited for this kind of austenitic stainless steel product to ensure that the products during the service still have enough plasticity and toughness [5].

The stress and strain parameters of 0Cr18Ni9 materials are obtained by tensile test. The stress and strain obtained by the experiment are called nominal stress and nominal strain. True stress and strain are needed during simulating the material plasticity parameter. Nominal stress σ_{nom} and strain ε_{nom} are transformed into true stress σ_{true} and strain $\varepsilon_{\text{true}}$ by

Table 1 The main parts of vacuum packaging machine

Number	Part name
1	Handle
2	Vacuum cover
3	Link
4	Seal assemble
5	Vacuum chamber
6	Chassis
7	Control panels
8	Caster

Table 2 Some characteristics of 0Cr18Ni9 material

Material	Elastic modulus/GPa	Poisson's ratio	Yield strength/MPa
0Cr18Ni9	204	0.285	205

$$\varepsilon_{\mathrm{nom}} = \frac{\Delta l}{l_0}, \tag{1}$$

$$\sigma_{\mathrm{nom}} = \frac{F}{A_0}, \tag{2}$$

$$\varepsilon_{\mathrm{true}} = \int_{l_0}^{l} \frac{\mathrm{d}l}{l} = \ln\left(\frac{l}{l_0}\right) = \ln(1 + \varepsilon_{\mathrm{nom}}), \tag{3}$$

$$\sigma_{\mathrm{true}} = \frac{F}{A} = \frac{F}{A_0 \frac{l}{l_0}} = \sigma_{\mathrm{nom}}(1 + \varepsilon_{\mathrm{nom}}). \tag{4}$$

The relationship between true stress and strain is shown in Fig. 2.

The vacuum chamber manufacturing process consists of laser cutting, bending and welding. Of course, there is another way to build the vacuum chamber through the stud welding technology which is more advanced and high efficiency [7]. As the vacuum chamber is the center of the symmetrical pattern and most of the vacuum chamber manufacturing process are welding, 1/4 model for simulation that can get the same accuracy on the simulation result is constructed to save time and improve efficiency, as shown in the Fig. 3.

When one dimension scale is much smaller than other components, FEA can be carried out using shell element to simplify the calculation. At present, the solid shell

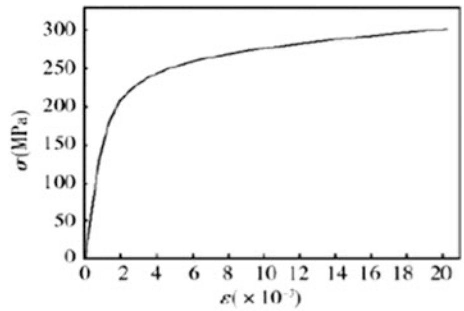

Fig. 2 The stress strain curve [6]

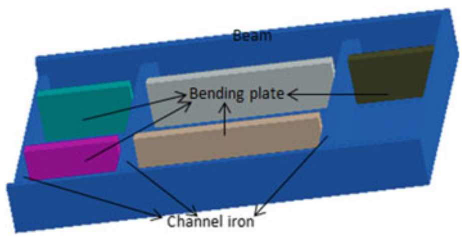

Fig. 3 The 1/4 model of vacuum chamber

element has aroused widespread concern [8]. The shell element is divided into three categories: general shell, thin shell and thick shell. It is generally considered that if the ratio of thickness to span of the shell which is made of a single material is between 1/20 and 1/10, it is thick shell. Because the vacuum chamber thickness is only 4 mm, much smaller than 1/10 of global size belongs to the typical shell element. So it is necessary to extract the thin shell of the vacuum chamber. The features of the suction holes, threaded holes and so on are ignored to reduce the calculation. The Visual Mesh software is used to clean up the geometry and repair the surface, as well as to complete the surface modeling. The replanting size is 10 which is greater than thickness. The fine meshes are adopted in the diagonal to improve the accuracy of computation and the coarse meshes are used in less important regions where they don't have problems to reduce the solution time. The density of mesh has little impact on the mechanical response of crystal plastic deformation and the mesh quality can be used to analyze three-dimensional elasticity problems [9, 10]. The meshing model is shown in Fig. 4.

The appropriate thickness and assignment material for various parts of the shell is set according to the thickness of the plate and ribs [11]. The purpose of applying the boundary constraint is to prevent the rigid displacement during calculation [12]. Boundary conditions are based on the actual working conditions. The vacuum chamber is fixed at four sides as a fixed constraint. There are 13 welds, the welding wizard is set according to the number on the grid model. All of the pretreatments are processed by Visual Weld. The corresponding stress results are shown in Fig. 5.

The stress result with a maximum stress of 350.5 MPa is shown in Fig. 5. The stress level is high and it exceeds the yield strength of the material. It is seen that stress concentrates in the bending plate and the channel junction. The stress concentration is the main factor affecting the fracture and maybe microstructure [13, 14]. The test machine shows the location of the crack. A path is built on the first weld to research the relationship between residual stress and yield strength. The red line is residual stress line and the green line is yield strength line. The result is shown in Fig. 6.

It is seen that there is a large fluctuation in residual stress and yield strength at each channel from Fig. 6. Especially, when there is a large increase in yield strength

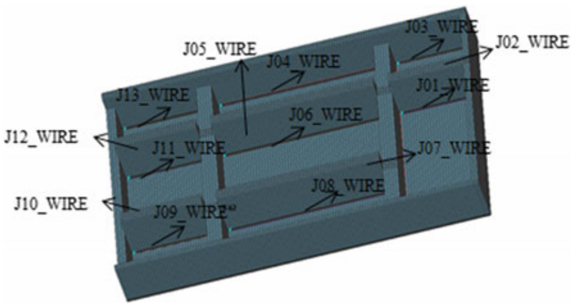

Fig. 4 The 1/4 model of the original vacuum chamber grid

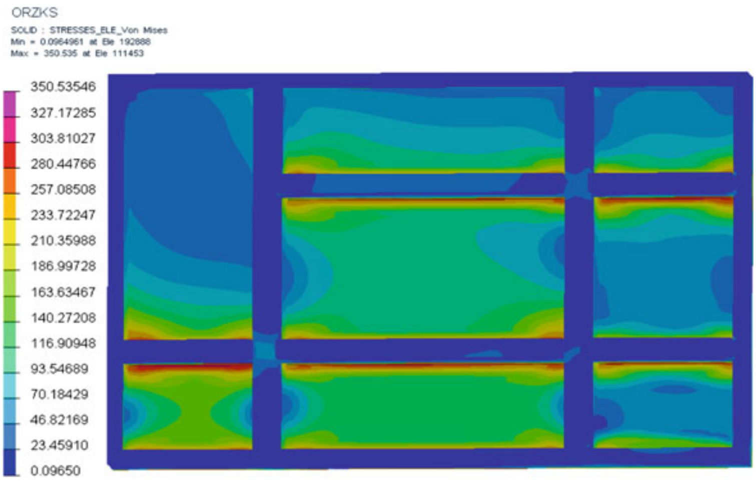

Fig. 5 The stress cloud of the vacuum chamber

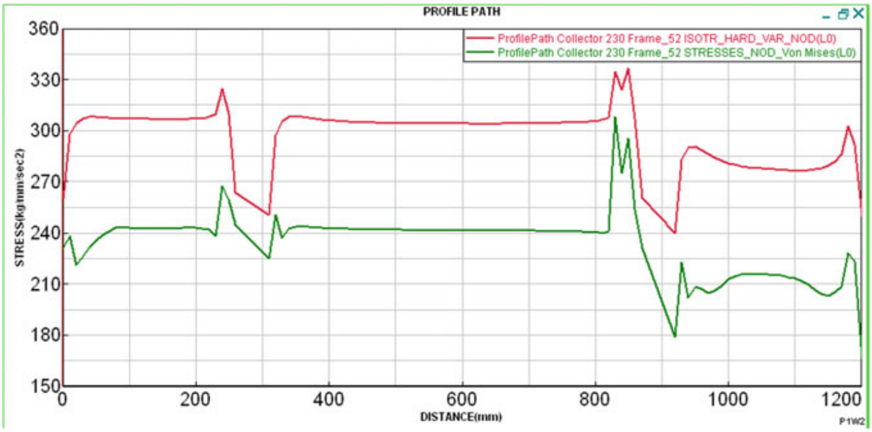

Fig. 6 The relationship between residual stress and yield strength for the vacuum chamber

at each channel and then there is a low fast drop, the residual stress changes slowly. There is no yield point but the residual stress and yield strength are very close. It is possible to cause material failure especially in the vacuum chamber of the studio because the vacuum state is easy to cause greater stress damage. As the number of welds increases, the much more residual stress is accumulated at the first weld. The load on the junction between channel iron and bending plate is mainly shared by the bending plate. Large stress is concentrated in their junction and it easily causes weld cracks.

The cause of junction stress for channel iron and bending plate is considered: in commissioning model, the bending plate height is improved to improve the vacuum chamber stiffness in design. However, the increase of the bending plate height leads to fluctuation in the junction, which produces stress non-uniform and causes stress concentration and plastic deformation. The more the welds are, the worse the condition will be. As the number of welds increases, the much more stress is concentrated at the first weld.

3.2 Improved Vacuum Chamber

The test machine model is constructed and the possible cracking of the issues are proposed to improve the vacuum packaging machine program. The improved program especially aims at bending plate and reducing the welds. It is not by the use of welding but the mechanical methods for the vacuum chamber of the central beam. The bending plate height is reduced through 45° treating at the end of bending plate so that the junction channel iron has uniform stress. The improved model is shown in Fig. 7. The same way is used to mesh the improved vacuum chamber and the grid model is shown in Fig. 8.

The same method is used to analyze the improved vacuum chamber. Because it is not by the use of welding but the mechanical methods for the vacuum chamber of the central beam, the number of welds reduces to 10. Compared with the previous model, this model has decreased three welds. The overall model will reduce 12 welds due to only a 1/4 of the present model. The less welds will shorten the product completion time and improve the efficiency for the enterprises. The same method is used to make all pretreatments, and then the file is put to simulate. The corresponding result is shown in Fig. 9.

The stress is shown on the border of improved model and significant improvement is got. There is a slight decrease in the maximum stress and the maximum value is decreased from previous 350.5 to 312.9 MPa. The position of the maximum stress has changed and the maximum stress concentration area

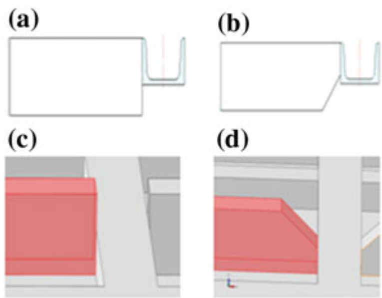

Fig. 7 The comparison chart of bending plate before and after improvements: the original bending plate (**a**); the improved bending plate (**b**); the original three-dimensional model (**c**); the improved three-dimensional model (**d**)

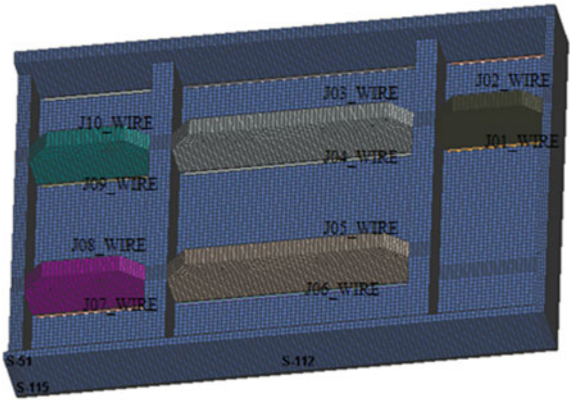

Fig. 8 The 1/4 model of the advanced vacuum chamber grid

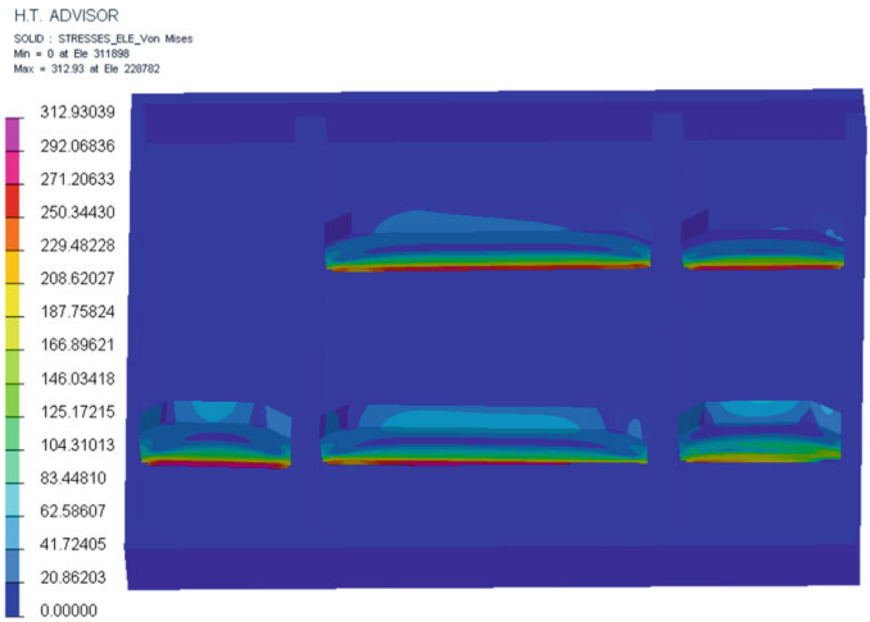

Fig. 9 The stress cloud of the improved vacuum chamber

decreases significantly while the stress distribution has improved a lot. The same path from top to bottom is built on the first weld to research the path change relationship between residual stress and yield strength. The location of the path is the same as that of the test machine's vacuum chamber, as shown in Fig. 10.

The overall variation curve is consistent with the previous model. The stress is improved and the maximum value is reduced from previous 340 to 310 MPa, about

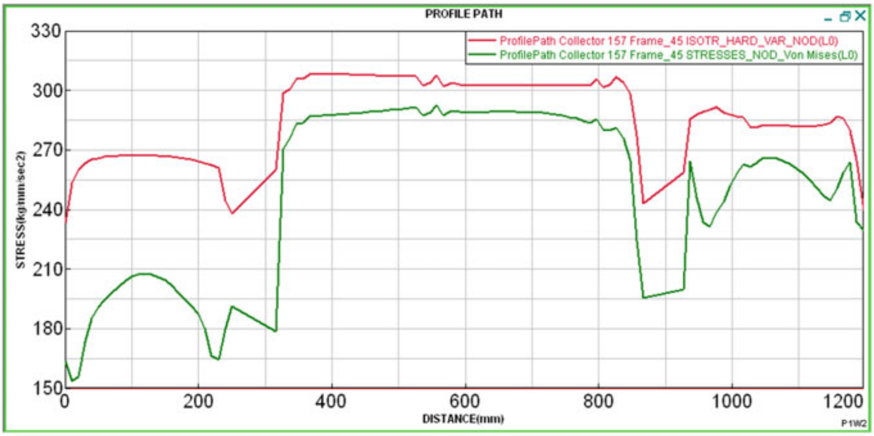

Fig. 10 The relationship between residual stress and yield strength for the improved vacuum chamber

9%. It can be known that the method of reducing welds is working. Compared with those of the vacuum chamber of tested machine, the residual stress and yield strength change slowly. It can be deduced from Fig. 10 that the stress of each channel just decreases, not increases. There is a certain stress reduction at the junction and the amplitude of fluctuation is relatively small. In each junction, the stress value is reduced. It shows that the improved channel iron can play a better supporting role. Bending plate can share the load better.

It is also known that the stress value at the junction of the channel and the bending plate in the previous stress analysis is the greatest. It is also possible to infer from Fig. 11. Although the stress value is the largest here in the improved model, the stress is much large in the yield curve from the yield strength. So the modified model to improve the stress of this position plays an important role.

In order to research the relationship between stress and yield strength at the original and improved models, a path in the channel and the first weld at the bending plate are established. The result is shown in Fig. 11. It can be seen that the residual stress of the original model is fluctuant. While the residual stress of the improved model steadily reduces. The residual stress and yield strength are obviously lower than those of original model. So the improved model is less likely to yield and has better performance.

4 Conclusion

FEA of the 1/4 vacuum chamber is used to distinguish the positions where stress is large and relatively concentrated and the stress amplitude changes greatly. These areas can produce plastic deformation which influences the quality of products

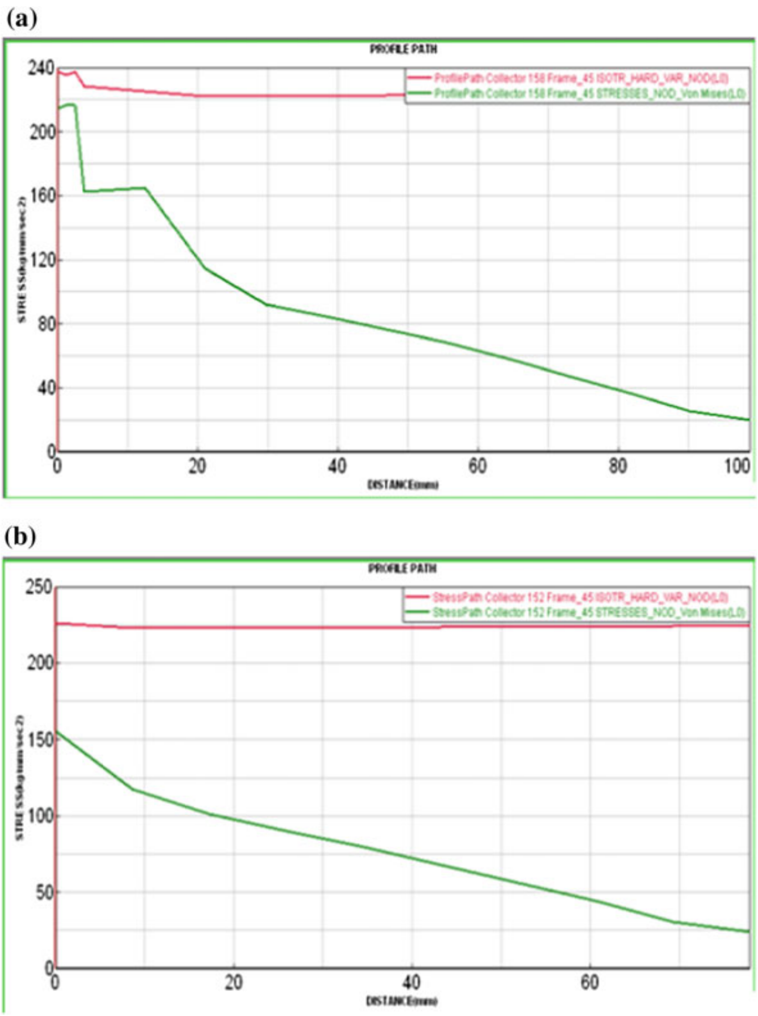

Fig. 11 The relationship between residual stress and yield strength at the position of channel and bend plate junction: original model (**a**) and advanced model (**b**)

seriously. In order to improve the bending plate with 45° treat at the end of bending plate and to reduce the welds, it is not by the use of welding but the mechanical methods for the vacuum chamber of the central beam. It can be deduced that the stress of the improved vacuum chamber has decreased by FEA. At the same time, a path for a particular site is constructed where the range of stress changes from the original 270–340 to 240–310 MPa and the stress is greatly improved. The actual effect will be more obvious if the simulation model is overall. The results of the simulation provide theoretical basis for improving the vacuum chamber structure.

Acknowledgements This work is supported by the National Natural Science Foundation of China (51575401) and the Zhejiang Provincial Natural Science Foundation (LY16E050007).

References

1. Sun JM, Li Z (2014) Design and study on the deoxidizing system in antioxidant packaging equipment. Packag Eng 35(7):6–10
2. Wang YH, Chen XZ, Huang L et al (2016) Finite element analysis and improvement of vacuum cover for packing machine. J Shanghai Jiao Tong Univ 50(12):1925–1928
3. Han C, Kim KS (2001) Time-dependent crack growth in stainless steel 304 in the plasticity-dominant field. Eng Fract Mech 68(1):39–52
4. Baik YM, Kim KS (2001) The combined effect of frequency and load level on fatigue crack growth in stainless steel 304. Int J Fatigue 23(5):417–425
5. Ling L, Li XX, Wang XL et al (2012) Constitutive model of stainless steel OCr18Ni9 and its influence on cutting force prediction. China Mech Eng 23(18):2243–2247
6. Li XM (2012) Study on plastic deformation behavior of stainless steel 0Crl8Ni9Ti under uniaxial stress. CFHI Technol 2:46–49
7. Wang YH, Chen XZ, Jiang Q (2016) Pull arc stud welding process of the vacuum chamber of the double chamber vacuum packaging machine. Weld Technol 45(5):119–122
8. Hauptmann R, Doll S, Harnau M et al (2001) “Solid-shell” elements with linear and quadratic shape functions at large deformations with nearly incompressible materials. Comput Struct 79(18):1671–1685
9. Kanber B, Bozkurt OY (2006) Finite element analysis of elasto-plastic plate bending problems using transition rectangular plate elements. Acta Mech Sin 22(4):355–365
10. Guzelbey IH, Kanber B (2000) A practical rule for the derivation of transition finite elements. Int J Numer Meth Eng 47(5):1029–1056
11. Yang L, Kong FY, Wang W (2014) Numerical simulation for temperature effect of external thermal insulation system with XPS board. J Shenyang Univ Technol 36(6):701–705
12. Wang YH, Chen XZ, Konovalov S (2016) Strain-stress simulation and comparison of different welding sequences during manufacturing of packing vacuum cover. Series Mater Sci Eng 150(1):012036
13. Li QF (2004) Fracture mechanics and engineering applications. Harbin Engineering University Press, Harbin, China
14. Fang YY, Chen XZ, Bruce M et al (2016) Effects of strain rate on the hot deformation behavior and dynamic recrystallization in China low activation martensitic steel. Fusion Eng Des 103:21–30